

# Process $e^+e^- \rightarrow \pi^0\pi^0\gamma$ at the energy range of about 1 GeV

M.N.Achasov, V.M.Aulchenko, A.V.Berdyugin, A.V.Bozhenok, D.A.Bukin, S.V.Burdin, T.V.Dimova, V.P.Druzhinin, M.S.Dubrovin, I.A.Gaponenko, V.B.Golubev, V.N.Ivanchenko, I.A.Koop, A.A.Korol, S.V.Koshuba, E.V.Pakhtusova, V.V.Shary, S.I.Serednyakov, Yu.M.Shatunov, V.A.Sidorov, Z.K.Silagadze<sup>a</sup>, A.A.Valishev

<sup>a</sup>Corresponding author, e-mail silagadze@inp.nsk.su, Fax +7 3832 35 21 63

$e^+e^- \rightarrow \omega\pi^0 \rightarrow \pi^0\pi^0\gamma$  reaction was investigated in SND experiment at VEPP-2M collider. A narrow energy interval near  $\phi$ -meson was scanned. The observed cross-section reveals, at the level of three standard deviation, the interference effect caused by  $\phi \rightarrow \pi^0\pi^0\gamma$  decay. The cross-section parameters, as well as the real and imaginary parts of the  $\phi$ -meson related amplitude, were measured.

## 1. Introduction

Experimental study of the  $e^+e^- \rightarrow \omega\pi^0$  reaction is interesting because of the following reasons [1,2]:

- Radial excitations of  $\rho$ -meson should reveal themselves in this reaction.
- A significant deal of the total cross section of  $e^+e^-$  annihilation into hadrons is determined by the  $\omega\pi^0$  intermediate state.
- The  $\omega\rho\pi$  vertex, which is dominant in the  $e^+e^- \rightarrow \omega\pi^0$  transition, appears also in a number of hadron decays, like  $\omega \rightarrow 3\pi$ ,  $\omega \rightarrow \pi^0\gamma$ ,  $\rho \rightarrow \pi\gamma$ ,  $\omega \rightarrow \mu^+\mu^-\pi^0$ ,  $\pi^0 \rightarrow 2\gamma$ . The precise experimental data about these processes stimulate theoretical study of the underlying hadron dynamics.

The  $e^+e^- \rightarrow \omega\pi^0$  transition can be studied in either  $e^+e^- \rightarrow \omega\pi^0 \rightarrow \pi^+\pi^-\pi^0\pi^0$  or  $e^+e^- \rightarrow \omega\pi^0 \rightarrow \pi^0\pi^0\gamma$  channels. The latter is more preferable concerning background conditions.

$e^+e^- \rightarrow \omega\pi^0 \rightarrow \pi^0\pi^0\gamma$  reaction in the energy range 1.0 ÷ 1.4 GeV was studied earlier by ND detector [1,2]. Indirectly, the  $\sigma(e^+e^- \rightarrow \omega\pi^0)$  cross section was extracted also from the ARGUS data on  $\tau^- \rightarrow \nu_\tau\omega\pi^-$  decay [3], under assumption of the Conserved Vector Current (CVC). The results are in good agreement, so confirming CVC hypothesis.

Since 1995, a new set of experiments began by the SND detector [4] on Novosibirsk VEPP-2M storage ring [5].

Below we report the results on  $e^+e^- \rightarrow \omega\pi^0 \rightarrow \pi^0\pi^0\gamma$  reaction, based on 1996-1997 two-year SND statistics.

## 2. Cross section estimate

The expected cross section is estimated using simple phenomenological, vector meson dom-

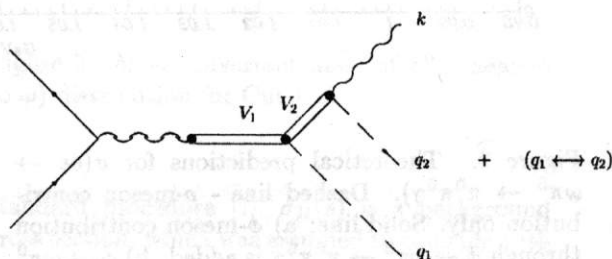


Figure 1.  $e^+e^- \rightarrow \pi^0\pi^0\gamma$

inance based, model (Fig.1).

Coupling constants and  $\phi$ - $\rho$ - $\omega$  mixing parameters were estimated using experimental data on various processes. The expected cross section is shown on Fig.2. Note the significant interference effect near  $\phi$  meson.

## 3. Event selection

Data sample, which was analyzed, corresponds to the integrated luminosity of  $4.5 pb^{-1}$ , collected by SND in the narrow energy interval near the  $\phi$ -meson.

For the reaction

$$e^+e^- \rightarrow \omega\pi^0 \rightarrow \pi^0\pi^0\gamma, \quad (1)$$

the possible sources of background are the following processes

$$\bullet e^+e^- \rightarrow \phi \rightarrow \eta\gamma \rightarrow 3\pi^0\gamma \quad (2)$$

$$\bullet e^+e^- \rightarrow \phi \rightarrow K_S K_L \rightarrow \text{neutral particles} \quad (3)$$

$$\bullet e^+e^- \rightarrow \phi \rightarrow f_0\gamma \rightarrow \pi^0\pi^0\gamma \quad (4)$$

Primary selection of the  $e^+e^- \rightarrow \omega\pi^0 \rightarrow \pi^0\pi^0\gamma$  candidates was done according to following criteria:

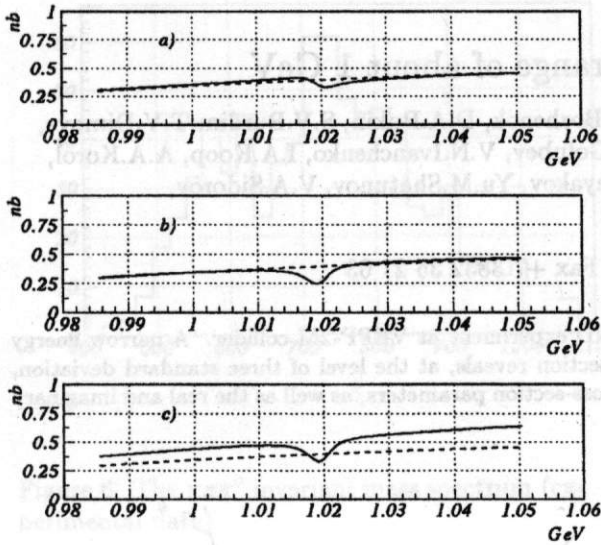


Figure 2. Theoretical predictions for  $\sigma(ee \rightarrow \omega\pi^0 \rightarrow \pi^0\pi^0\gamma)$ . Dashed line -  $\rho$ -meson contribution only. Solid line: a)  $\phi$ -meson contribution through  $\phi \rightarrow \rho\pi^0 \rightarrow \pi^0\pi^0\gamma$  is added. b)  $\phi \rightarrow \omega\pi^0$  transition due to  $\rho$ - $\omega$ - $\phi$  mixing is also included in the  $\phi$ -meson contribution. c)  $\rho'$ -meson contribution is added to the above ones.

- event must contain exactly 5 photons in the calorimeter and have no charged particles.
- azimuth angle of any final photon lies within the interval  $27^\circ < \theta < 153^\circ$ .
- total(normalized over  $2E$ ) energy deposition of final photons is in the range  $0.8 \leq E_{tot}/2E \leq 1.1$ .
- normalized full momentum of the event ( $P_{tot}/2E$ ) is less than 0.15.

After this primary selection, our 5-photon events are predominantly  $2\pi^0$  events also, as Fig.3 indicates. On this figure a combined 2-dimensional plot of invariant masses of some photon pairs ( $M_{24}$  versus  $M_{35}$  plus  $M_{25}$  versus  $M_{34}$ , photons are arranged according to their energy, the most energetic being the first one) is shown. This figure also illustrates that background (2) produces a wider distribution. This can be used for rejection of this background. Namely, kinematic fit was performed for each 5-photon event under assumption that there are two  $\pi^0$ -s in the final state and energy-momentum balance holds within experimental accuracy.  $\chi^2$  of this fit ( $\chi_{\pi^0\pi^0\gamma}^2$ ) was used for the background rejection.

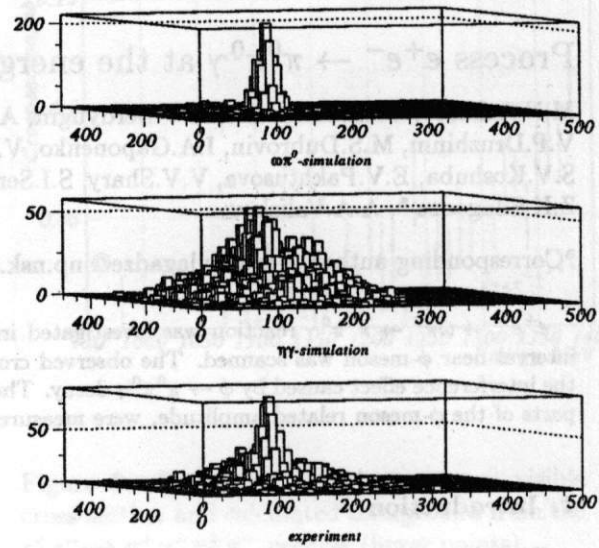


Figure 3.  $M_{24}$  versus  $M_{35}$  added by  $M_{25}$  versus  $M_{34}$

Background from (2) simulates  $\pi^0\pi^0\gamma$  events mainly due to loss of photons through the openings in the calorimeter around detector poles and/or merging of close photon pairs. When photons merge in the calorimeter, the corresponding electromagnetic shower is, as a rule, broader in transverse direction, than the electromagnetic showers from the normal single photons. This circumstance can be used to discriminate merged photons and so a great deal of background (2). The corresponding parameter ( $\zeta_\gamma$ ) is described in [6]. A 2-dimensional distributions of our events in the  $\chi_{\pi^0\pi^0\gamma}^2, \zeta_\gamma$  plane, as well as Monte-Carlo simulated (1) signal events and (2) background events (Fig.4), indicate that our signal events are almost completely bound in the  $\zeta_\gamma < 20$ ,  $\chi_{\pi^0\pi^0\gamma}^2 < 40$  area.

On the base of this considerations, we have chosen the following two sets (Cut I and Cut II) of selection criteria for the channel (1) separation (in addition to the primary selection rules, described above):

- normalized full momentum of the event is less than 0.1 (for Cut I).
- there are two  $\pi^0$ -mesons in the event, that is one can find two distinct pairs of photons with invariant masses within  $\pm 30$  MeV from the  $\pi^0$ -mass.
- $\chi_{\pi^0\pi^0\gamma}^2, \chi^2$  of the kinematic fit, is less than 20 for Cut I, or is less than 40 for milder Cut II.

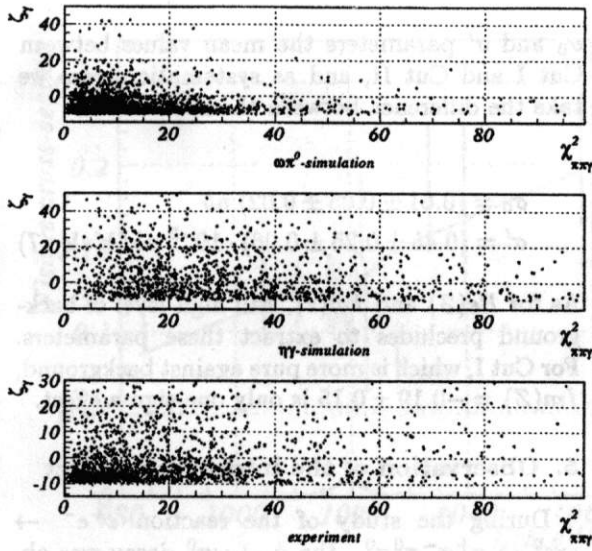


Figure 4.  $\zeta_\gamma$  versus  $\chi^2_{\pi^0\pi^0\gamma}$  distributions.

- $\zeta_\gamma$ , the parameter describing the transverse profile of the electromagnetic shower, is less than 0 for Cut I, or is less than 20 for Cut II.

Recoil mass of the photon from the background reaction (4) is peaked at the  $f_0$ -meson mass and this peculiarity can be used to separate a great deal of such events from the events of reaction (1). We have chosen  $M_\gamma < 700\text{MeV}$  condition as one more cut to select events from the process (1), where  $M_\gamma$  stands for the photon recoil mass.

After applying these cuts, the  $\omega$ -meson peak is clearly seen in the invariant mass of  $\pi^0$  and  $\gamma$  (for each  $\pi^0\pi^0\gamma$  event, from two possible  $(\pi^0, \gamma)$  combinations, the one is taken, which has  $M_{\pi^0\gamma}$  closest to  $M_\omega$ ), as it is illustrated by Fig.5. Finally, to extract channel (1),  $750\text{MeV} < M_{\pi^0\gamma} < 820\text{MeV}$  condition was added to the above mentioned cuts.

The distributions for all parameters, used in event selections, show good agreement between MC and experiment. As an example, in Fig.6 we present  $M_{\pi^0\gamma}$  distributions.

#### 4. Data analysis and results

We assume the following parameterization for the visible (detection) cross section  $\sigma_v$ :

$$\sigma_v = \epsilon[1 + \delta(s)]\sigma(s) + kb\sigma_B(s), \quad (5)$$

where  $\epsilon$  is the detection efficiency for the process (1),  $\delta(s)$  accounts for the radiative corrections, which are calculated according to the

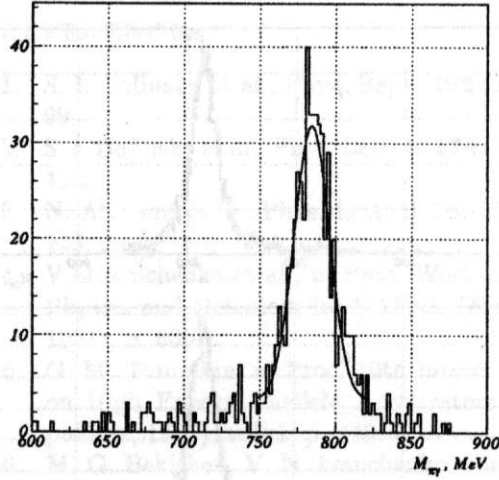


Figure 5.  $M_{\pi^0\gamma}$  (invariant mass of  $\pi^0\gamma$ , nearest to  $\omega$ ) distribution for Cut I

standard procedure [7],  $\sigma_B(s)$  is a background cross section, which was assumed to coincide with  $\sigma(e^+e^- \rightarrow \eta\gamma \rightarrow 3\pi^0\gamma)$ ,  $k$  is the background suppression factor. To take into account other  $\phi$ -meson related backgrounds, factor  $b$  is introduced in (5). It is assumed that the different energy dependencies of various background cross-sections is not relevant at the present level of statistical accuracy and so they all can be approximated by  $\sigma(e^+e^- \rightarrow \eta\gamma)$  behavior. At last,  $\sigma(s)$  is a cross section of the process under investigation. Because we are interesting for  $\sigma(s)$  in a narrow energy interval, we have taken

$$\sigma(s) = [\sigma_0 + \sigma'(2E - M_\phi)]|R|^2, \quad (6)$$

$$R = 1 - Z \frac{m_\phi \Gamma_\phi}{s - M_\phi^2 + iM_\phi \Gamma_\phi}.$$

The detection efficiency  $\epsilon$  was calculated using Monte-Carlo simulation in conditions of individual scans for various energies. Detection efficiencies do not show any significant energy dependence. So we have taken an averaged over scans and energies efficiency  $\epsilon = (29.7 \pm 0.25)\%$  (only statistical error is indicated) as a fair estimate for Cut II.

For a tighter Cut I some systematic errors could be expected. To estimate this systematics, we compared the numbers of rejected events for each parameter of Cut I. It was found that, in total, the Monte Carlo simulation  $1.12 \pm 0.06$  times overestimates the detection efficiency, if we assume that there are no correlations between used selection parameters. With this correction factor taken into account, the averaged detection effi-



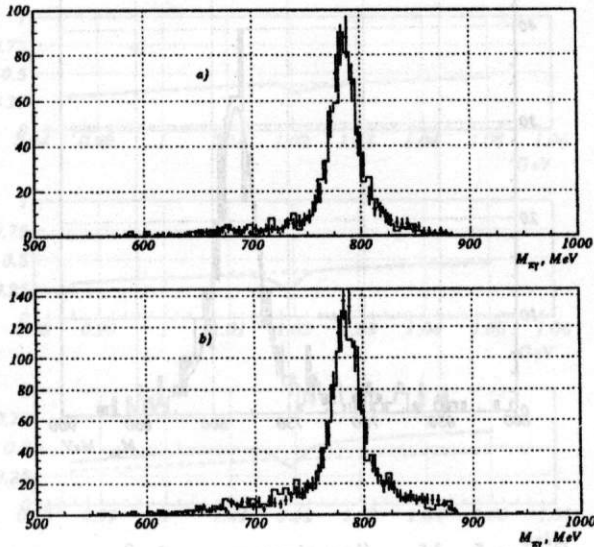


Figure 6.  $M_{\pi^0\gamma}$  distributions : MC simulation (points with error bars) and experiment (histogram). a) for Cut I and b) for Cut II

Table 1  
Fitted parameters for the fit with the interference

parameter	Cut I	Cut II
$\sigma_0$ (nb)	$0.60 \pm 0.05$	$0.62 \pm 0.05$
$\sigma' \cdot 10^2$ (nb/MeV)	$0.42 \pm 0.25$	$0.48 \pm 0.21$
$Re(Z)$	$0.1 \pm 0.1$	$0.12 \pm 0.08$
$Im(Z)$	$-0.19 \pm 0.15$	$0.04 \pm 0.08$
$b$	$2.6 \pm 1.7$	$0.1 \pm 0.3$
$\chi^2/d.f.$	11.1/10	14.6/10

lection parameters. With this correction factor taken into account, the averaged detection efficiency  $\epsilon = (20.7 \pm 1.1)\%$  was obtained for Cut I.

The background suppression factor  $k$  was also assumed to be energy independent. It was calculated by using  $\sim 2.15 \cdot 10^5$  simulated events from the process (2) and equals  $(2.7 \pm 0.3) \cdot 10^{-4}$  for Cut I and  $(1.10 \pm 0.06) \cdot 10^{-3}$  for Cut II.

The fit results are given in the Table 1.

As we see, results for Cut I and Cut II are consistent after the detection efficiency for Cut I is corrected against estimated systematics. Of course, we don't know if there are some amount of systematic errors left uncorrected for Cut I. On the other hand, for Cut II more background is expected and we can neither very precisely estimate this background (for example, the part coming from (3)) nor subtract it during fit.

Therefore we select as a fair estimates for the

$\sigma_0$  and  $\sigma'$  parameters the mean values between Cut I and Cut II, and as systematic errors we take the difference between them.

$$\sigma_0 = (0.61 \pm 0.05 \pm 0.02) \text{ nb}$$

$$\sigma' = (0.45 \pm 0.25 \pm 0.06) \cdot 10^{-2} \text{ nb/MeV} \quad (7)$$

As for  $Re(Z)$  and  $Im(z)$ , still high level of background precludes to extract these parameters. For Cut I, which is more pure against background,  $Im(Z) = -0.19 \pm 0.15$  is only one sigma effect.

## 5. Observation of the interference effect

During the study of the reaction  $e^+e^- \rightarrow \omega\pi^0 \rightarrow \pi^+\pi^-\pi^0\pi^0$ , the  $\phi \rightarrow \omega\pi^0$  decay was observed for the first time with the branching ratio about  $5 \cdot 10^{-5}$  [8]. The decay reveals itself as an interference wave on nonresonant cross section of the process  $e^+e^- \rightarrow \omega\pi^0$ . In principle, the similar picture should be observed in neutral channel (1). Really the whole situation here looks more complicated because of other  $\phi$  meson neutral decays like  $\phi \rightarrow \rho^0\pi^0$ ,  $\phi \rightarrow f_0\gamma$ ,  $\sigma\gamma$  [9], which have the same final state and interfere with the process (1). The interference amplitude with the  $\phi \rightarrow \rho^0\pi^0$  decay is expected to be about 10%, which is close to the value 17% due to  $\phi \rightarrow \omega\pi^0$  decay, obtained in [8]. In our preceding study [10] of the reaction (1), we did not observe the interference because of small statistics and nonresonant background.

In the present work the analysis given above also doesn't reveal the interference effect with certainty in spite of higher statistics, because the background is still high. In [8] another analysis, specially dedicated to the interference observation, was performed. The following parameters of the interference amplitude were obtained

$$Re(Z) = 0.036 \pm 0.052,$$

$$Im(Z) = -0.186 \pm 0.063. \quad (8)$$

The visible cross section under rather tight cuts of this analysis and fitted curve with  $\chi^2/d.f. = 11.9/11$  are shown on Fig.7. The fitted resonant background is also shown at the bottom. One could see, that in spite of imposed strong cuts, the resonant background is about one third of interference amplitude wave and is the dominant source of systematic error in Z.

## 6. Conclusions.

In conclusion, we obtained in the present work the following values of the  $e^+e^- \rightarrow \omega\pi^0 \rightarrow \pi^0\pi^0\gamma$

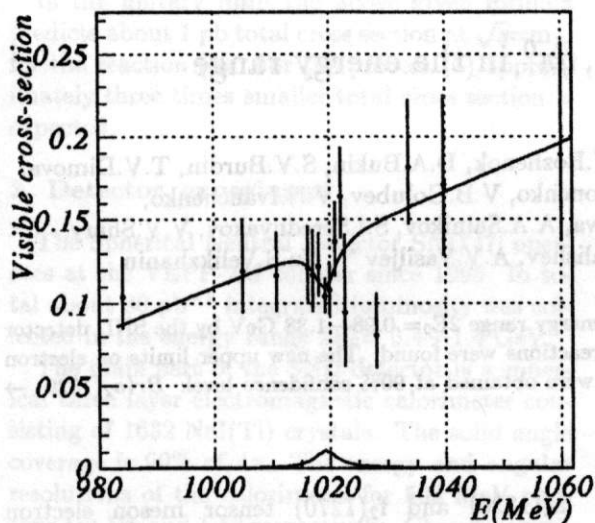


Figure 7. Visible cross-section for the process  $e^+e^- \rightarrow \omega\pi^0 \rightarrow \pi^0\pi^0\gamma$  under cuts of [8] and the optimal fit. The fitted resonance background is also shown at bottom.

process cross section parameters:

$$\begin{aligned} \sigma_0 &= (0.61 \pm 0.05 \pm 0.04) \text{ nb}, \\ \sigma' &= (0.0045 \pm 0.0025 \pm 0.0020) \text{ nb/MeV}, \\ \text{Re}(Z) &= 0.036 \pm 0.052, \\ \text{Im}(Z) &= -0.186 \pm 0.063. \end{aligned} \quad (9)$$

The measured nonresonant cross section  $\sigma(e^+e^- \rightarrow \omega\pi^0) = \sigma(e^+e^- \rightarrow \omega\pi^0 \rightarrow \pi^0\pi^0\gamma)/\text{Br}(\omega \rightarrow \pi^0\gamma) = (7.2 \pm 0.6 \pm 0.5) \text{ nb}$  agrees with the result  $(8.7 \pm 1.0 \pm 0.7) \text{ nb}$  from [1] and with the result  $(8.6 \pm 0.9) \text{ nb}$  from [8] in channel with charged pions  $e^+e^- \rightarrow \omega\pi^0 \rightarrow \pi^+\pi^-\pi^0\pi^0$ , as well as with the recent CMD-2 result [11]. This value of the nonresonant cross section can not be explained by only  $\rho$ -meson contribution and indicates significant effects from  $\rho$ -meson radial excitations. The measured interference amplitude [8] is three standard deviation above 0 and is consistent with the results for charged pions channel in the framework of the used theoretical model.

More detailed version of this work will be published.

## 7. Acknowledgement

This work is supported in part by Russian Fund for basic researches, grants No. 97-02-18561 and 96-15-96327.

## REFERENCES

1. S. I. Dolinsky et al., Phys. Rept. **202** (1991), 99.
2. S. I. Dolinsky et al., Phys. Lett. **B 174** (1986), 453.
3. N. Albrecht et al., Phys. Lett. **B 185** (1987), 223.
4. V.M. Aulchenko et al., in Proc. Workshop on Physics and Detectors for DAFNE (Frascati, 1991), p. 605.
5. G. M. Tumaikin, in Proc. 10th Intern. Conf. on High Energy Particle Accelerators (Serpukhov, 1977), vol. 1, p. 443.
6. M. G. Bekishev, V. N. Ivanchenko, Nucl. Instr. and Meth. **A 361** (1995), 138.  
A. V. Bozhenok, V. N. Ivanchenko, Z. K. Silagadze, Nucl. Instr. and Meth. **A 379** (1996), 507.
7. E. A. Kuraev, V. S. Fadin, Sov. J. Nucl. Phys. **41** (1985) 466.  
O. Nicrosini, L. Trentadue, Phys. Lett. **196B** (1987), 551.  
G. Bonneau, F. Martin, Nucl. Phys. **B27** (1971), 381.
8. M. N. Achasov et al., Novosibirsk preprint BUDKERINP-98-65 (hep-ex/9809013).
9. M. N. Achasov et al., hep-ex/9711023.  
V. M. Aulchenko et al, hep-ex/9807016.
10. M. N. Achasov et al., Novosibirsk preprint BUDKERINP-97-78 (hep-ex/9710017).
11. R. R. Akhmetshin et al., Novosibirsk preprint BUDKERINP-99-11.